Food Chemistry: X 14 (2022) 100288

Contents lists available at ScienceDirect

Food Chemistry: X

journal homepage: www.sciencedirect.com/journal/food-chemistry-x

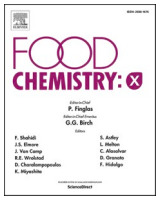

Dynamic variations in physicochemical characteristics of oolong tea polysaccharides during simulated digestion and fecal fermentation *in vitro*

Ding-Tao Wu [a,*], Wen Liu [b], Qin Yuan [b], Ren-You Gan [a,c], Yi-Chen Hu [a], Sheng-Peng Wang [b], Liang Zou [a,*]

[a] *Key Laboratory of Coarse Cereal Processing, Ministry of Agriculture and Rural Affairs, Sichuan Engineering & Technology Research Center of Coarse Cereal Industralization, School of Food and Biological Engineering, Chengdu University, Chengdu 610106, China*
[b] *State Key Laboratory of Quality Research in Chinese Medicine, Institute of Chinese Medical Sciences, University of Macau, Macao, China*
[c] *Research Center for Plants and Human Health, Institute of Urban Agriculture, Chinese Academy of Agricultural Sciences, Chengdu 610213, China*

ARTICLE INFO

Keywords:
Oolong tea
Polysaccharide
Physicochemical property
Simulated digestion
Fecal fermentation
Intestinal microbiota

ABSTRACT

In this study, dynamic variations in physicochemical characteristics of polysaccharides from 'Wuyi rock' tea (WYP) at different simulated digestion and fecal fermentation stages *in vitro* were studied. Results revealed that physicochemical characteristics of WYP were slightly altered after the simulated digestion *in vitro*, and its digestibility was about 8.38%. Conversely, physicochemical characteristics of the indigestible WYP, including reducing sugar, chemical composition, constituent monosaccharide, molecular weight, and FT-IR spectrum, were obviously altered after the fecal fermentation *in vitro*, and its fermentability was about 42.18%. Notably, the indigestible WYP could remarkably modulate the microbial composition *via* promoting the proliferation of profitable intestinal microbes, such as *Bacteroides*, *Lactococcus*, and *Bifidobacterium*. Moreover, it could also enhance the generation of short-chain fatty acids. The results showed that WYP was slightly digested in the gastrointestinal tract *in vitro*, but could be obviously utilized by intestinal microbiota, and might possess the potential to improve intestinal health.

1. Introduction

Tea is considered as one of the most popular beverages around the world, which is made from the fresh leaf of *Camellia sinensis*. Generally, teas are divided into five classifications in China based on the different processes, including green tea (un-fermented), white tea (slight-fermented), oolong tea (half-fermented), black tea (full-fermented), and dark tea (post-fermented) (Jiang et al., 2019). Oolong tea belongs to the half-fermented products of the fresh leaf of *C. sinensis*, which is widely consumed in south China and southeast Asia (Liu, Chen, Sun, & Ni, 2022). 'Wuyi rock' tea, one of the most famous and top-ranking subcategories of oolong tea, is famous for its typical 'rock flavor' of taste (Guo et al., 2021; Liu et al., 2022). Generally, polysaccharides extracted from teas have received increasing concerns owing to their promising health-beneficial properties (Chen et al., 2016; Xu et al., 2021), including anti-oxidant, anti-diabetic, anti-obesity, hepatoprotective, immunomodulatory, and anti-tumor effects, as well as regulation of gut microbiota. Specially, the anti-diabetic effect has attracted much attention because the tea beverage is widely consumed for the treatment of diabetes mellitus in Japan, Korea, and China. Polysaccharides extracted from oolong tea also possess remarkable antioxidant activity and anti-diabetic effect, which have been identified as acidic polysaccharides (Chen, Qu, Fu, Dong, & Zhang, 2009; Chen, Wang, et al., 2009; Guo et al., 2021; Wang et al., 2012; Xu et al., 2020). Nevertheless, studies on the polysaccharides extracted from 'Wuyi rock' tea are limited (Guo et al., 2021). Consequently, the study on physicochemical structures and bio-functions of polysaccharides from 'Wuyi rock' tea (WYP) is necessary, which is beneficial for further application of WYP as functional foods and functional ingredients.

Generally, the biological functions of dietary polysaccharides are closely associated with the metabolism from the stomach to the colon. In recent years, accumulating studies have focused on the digestive behavior and fermentation characteristic of dietary polysaccharides in the human gastrointestinal tract by using *in vitro* models involving mouth, stomach, small intestine, and large colon (Brodkorb et al., 2019; Guo et al., 2021; Li, Yu, Wu, & Chen, 2020; Wu, He, et al., 2021). Usually, dietary polysaccharides from natural resources can't be entirely digested or absorbed in stomach and small intestine, while can arrive to

* Corresponding authors.
E-mail addresses: wudingtao@cdu.edu.cn (D.-T. Wu), zouliang@cdu.edu.cn (L. Zou).

https://doi.org/10.1016/j.fochx.2022.100288
Received 18 January 2022; Received in revised form 16 March 2022; Accepted 17 March 2022
Available online 19 March 2022

large colon to be fermented by human intestinal microbes (Li et al., 2020; Wu, Fu, et al., 2021). Increasing experimental studies have proven that the indigestible dietary polysaccharides can benefit the host *via* promoting the growth of several beneficial bacterial, such as *Bacteroides*, *Lactobacillus*, and *Bifidobacterium*, and enhancing the generation of several metabolites by fermenting dietary polysaccharides, such as short-chain fatty acids (SCFAs) (Li et al., 2020; Liu, Li, Yang, Sun, & Cai, 2021; Wang, Li, Huang, Fu, & Liu, 2019; Wu, Yuan, et al., 2021). Indeed, SCFAs are associated with a low risk of metabolic syndromes (Rui et al., 2019; Wang et al., 2019). Therefore, dietary polysaccharides seem to exhibit several properties related to maintain host health, while the *in vitro* digestive behavior and fermentation properties of WYP, as well as its influence on the regulation of colonic microbial composition and the generation of SCFAs are still unclear. Consequently, it is necessary to clarify the potential digestive and fermented behaviors of WYP, which is helpful for promoting the design and production of functional foods based on WYP.

This study aimed to reveal the potential digestive and fermented behaviors of WYP by using an *in vitro* simulated digestion and fecal fermentation model. Besides, the effect of WYP on the modulation of colonic microbial composition was also evaluated.

2. Materials and methods

2.1. Materials and chemicals

'Wuyi rock' tea (Rougui) was purchased from Fujian Wu Yi Star Tea Industrial Co., Ltd. α-Amylase (1000 U/mg), bovine serum albumin (BSA), pepsin (3000 U/g), and pancreatin (4000 U/g) were purchased from Sigma-Aldrich (St. Louis, MO, USA). Inulin was purchased from Aladdin (Shanghai, China).

2.2. Preparation and isolation of polysaccharides from 'Wuyi rock' tea

Hot water extraction of polysaccharides from 'Wuyi rock' tea was performed as previously reported (Wu, Feng, et al., 2021). Firstly, the powders of 'Wuyi rock' tea (120.0 g) were treated with 1.2 L of ethanol (80%, *v/v*) at 80 °C for 2 h to remove several small molecules, such as phenolics and pigments. Subsequently, the extracted residues were treated with deionized water (1: 20, *w/v*) at 95 °C for 2 h. Polysaccharides from 'Wuyi rock' tea were then isolated by using graded alcohol precipitation and membrane separation. The precipitations treated with three volumes of ethanol (95%, *v/v*) were collected. Finally, polysaccharides extracted from 'Wuyi rock' tea (WYP) were dissolved, ultra-filtered (molar mass cutoff, 3.0 kDa) to further remove impurities, and freeze dried.

2.3. Simulated digestion of WYP

The simulated digestion of WYP was performed as the procedures described in the literature with minor modifications (Brodkorb et al., 2019). Firstly, KCl (15.1 mM), $CaCl_2(H_2O)_2$ (1.5 mM), $MgCl_2(H_2O)_6$ (0.15 mM), KH_2PO_4 (3.7 mM), $(NH_4)_2CO_3$ (0.06 mM), $NaHCO_3$ (13.6 mM), and HCl (1.1 mM) were mixed in the simulated salivary fluid. The mixtures of 100.0 mL of the WYP solution (20.0 mg/mL), 15 mg of α-amylase (1000 U/mg), and 100.0 mL of the simulated salivary fluid were blended and incubated at 37 °C (pH = 7.0). During the salivary digestion, 2.0 mL of the mixture was collected at the digested points of 0.25, 0.5, and 1.0 h for further analysis. Secondly, KCl (6.9 mM), $CaCl_2(H_2O)_2$ (0.15 mM), $MgCl_2(H_2O)_6$ (0.12 mM), KH_2PO_4 (0.9 mM), $(NH_4)_2CO_3$ (0.5 mM), $NaHCO_3$ (25.0 mM), NaCl (47.2 mM), and HCl (15.6 mM) were mixed in the simulated gastric fluid. The mixtures of 150.0 mL of the salivary digestion, 0.2 g of pepsin (3000 U/g), and 150.0 mL of the simulated gastric fluid were blended and quickly regulated to pH = 3.0 to trigger the simulated gastric digestion. 2.0 mL of the mixture was also collected for further analysis after 0.5, 1.0, 2.0, and 4.0 h of incubation at 37 °C. Finally, KCl (6.8 mM), $CaCl_2(H_2O)_2$ (0.6 mM), $MgCl_2(H_2O)_6$ (0.33 mM), KH_2PO_4 (0.8 mM), $NaHCO_3$ (85.0 mM), NaCl (38.4 mM), and HCl (8.4 mM) were mixed in the simulated intestinal juice. The mixtures of 180.0 mL of the digested sample, 1.47 g of bile salts, 1.8 g of pancreatin (4000 U/g), and 180.0 mL of the simulated intestinal juice were blended and quickly adjusted to pH = 7.0 to trigger the simulated intestinal digestion. Then, 2.0 mL of the mixture was also obtained for further analysis after 0.5, 1.0, 2.0, and 4.0 h of incubation at 37 °C.

All collected samples were firstly applied for the measurement of reducing sugar contents (C_R), and then sequentially treated by ethanol, ultra-filtered (3.0 kDa), and freeze dried. Samples of WYP digested at different digestion stages, including salivary, saliva-gastric, and saliva-gastrointestinal digestions, were collected and coded as WYP-S, WYP-G, and WYP-I, respectively.

2.4. Microbial fermentation of the indigestible WYP (WYP-I) by human feces

The fecal fermentation of the indigestible WYP (WYP-I) by human feces was also performed as previously reported (Wu, Yuan, et al., 2021), and the basic culture medium was prepared as described in the literature. Fresh feces were provided from two female and two male volunteers (ages from 18 to 25), they did not take any antibiotics and did not have digestive diseases. Fresh feces were mixed with the sterilized modified saline solution to prepare the fecal slurry (10%, *w/v*). The final human fecal inoculum was the supernatant of the fecal slurry after centrifugation. The WYPI group contained 1.0 mL of the human fecal inoculum and 9.0 mL of basic culture medium with 100.0 mg of WYP-I, which was carried out in penicillin bottles. The negative control (BLANK group) only contained the human fecal inoculum and the basic culture medium. The positive control (INULIN group) contained the human fecal inoculum, the basic culture medium, and 100.0 mg of inulin. Then, all groups were cultivated in an anaerobic condition at 37 °C.

Finally, different fermented samples were firstly applied for the detection of C_R, total polysaccharides, SCFAs, and free monosaccharide released. Additionally, fermented samples were sequentially treated by ethanol and ultra-filtered (molar mass cutoff, 3.0 kDa). Wuyi rock tea polysaccharides fermented at different time points of 6, 12, 24, and 48 h were obtained, and named as WYPI-6, WYPI-12, WYPI-24, and WYPI-48, respectively.

2.5. Measurement of variations in physicochemical characteristics of polysaccharides from 'Wuyi rock' tea at different digestive and fermented stages in vitro

2.5.1. Measurement of C_R, digestibility, fermentability, and chemical composition

The 3,5-dinitrosalicylic acid method was utilized to analyze the C_R released from WYP at different digestion stages *in vitro* and different fermented stages *in vitro*. Besides, the *m*-hydroxydiphenyl and phenol–sulfuric acid methods were applied for the measurement of total polysaccharides and total uronic acids as previously reported (Wu et al., 2022), respectively. The digestibility (%) of WYP at different digestion stages *in vitro* was calculated based on reducing sugars, and the fermentability (%) of WYP-I at different fermented stages *in vitro* was calculated based on total sugars and reducing sugars (Wu, Yuan, et al., 2021).

2.5.2. Measurement of free sugars released and monosaccharide composition

Free sugars released from WYP-I after the *in vitro* fermentation by human feces were analyzed by UltiMate U3000 LC system (Thermo Fisher Scientific, Waltham, MA, USA). A phenomenex gemini C18 110A column (150 mm × 4.6 mm, 5 μm) was used to separate free sugars released (Wu et al., 2022). Besides, monosaccharide compositions of

WYP at different digestion stages *in vitro* and WYP-I at different fermented stages *in vitro* were also measured by UltiMate U3000 LC system, respectively.

2.5.3. Measurement of molecular weights

Molecular weights (M_w) of WYP, WYP-S, WYP-G, WYP-I, WYPI-6, WYPI-12, WYPI-24, and WYPI-48 were measured by using size exclusion chromatography as previously reported (Wu et al., 2022). Both laser light scattering detection (MALS) and refractive index detector (RID) (Wyatt Technology Co., Santa Barbara, CA, USA) were utilized for the detection of polysaccharides' signals. The Shodex OHpak SB-G 6B (50 mm × 6.0 mm, i.d.) and the Shodex OHpak SB-806 M HQ (300 mm × 8.0 mm, i.d.) columns were applied for the separation of WYPs.

2.5.4. Spectrometric analysis

The FT-IR spectra of WYP, WYP-S, WYP-G, WYP-I, WYPI-6, WYPI-12, WYPI-24, and WYPI-48 were recorded by a Nicolet iS 10 FT-IR (Thermo Fisher Scientific, Waltham, MA, USA). Besides, the esterification degree (DE) values were also calculated based on the FT-IR spectra as previously reported (Wu, Feng, et al., 2021).

2.6. Analysis of gut microbial composition and short chain fatty acids (SCFAs)

The extraction, PCR amplification, purification, and sequencing of the bacterial 16S rRNA genes of the fermented mixture were performed as previously reported (Wu, Nie et al., 2021). Besides, the obtained data were also processed and analyzed as previously reported (Wu, Nie et al., 2021). Furthermore, an Agilent GC system (Agilent Technologies, Santa Clara, CA, USA) equipped with an Agilent HP-INNOWAX column (30 m × 0.25 mm × 0.25 μm) and a flame ionization detector was used to measure the contents of SCFAs in each fermented broth as formerly reported (Wu, Nie et al., 2021).

2.7. Statistical analysis

All experiments were run in triplicate. The results were expressed as mean ± standard deviations using Origin 9.0 software. Statistical significance was evaluated by the independent-sample *t*-test and one-way analysis of variance (ANOVA) plus *post hoc* Duncan's test (SPSS software, version 24.0).

3. Results and discussion

3.1. Dynamic variations in physicochemical characteristics of WYP at different simulated digestion stages in vitro

3.1.1. Dynamic variation in chemical composition

As shown in Table 1, the content of total polysaccharides in WYP was 83.49% ± 1.35%, which changed to 79.25% ± 1.58% after the *in vitro* simulated digestion, similar to the previously reported results that the total polysaccharides in chrysanthemum tea polysaccharides slightly declined after the *in vitro* digestion (Wu, Yuan, et al., 2021). Besides, the content of uronic acids in WYP was 43.33% ± 1.08%, which was similar to that of polysaccharides extracted from oolong tea (Tieguanyin, 45.89%) (Wang et al., 2012). After the *in vitro* simulated digestion, the content of uronic acids in WYP was overall stable. However, the obvious reduction of total polysaccharides in WYP might be caused by the acidic pH in the simulated digestion conditions (Huang et al., 2020).

3.1.2. Dynamic variation in molecular weight

As shown in Fig. 1A, a single polysaccharide fraction eluted from 17 to 21 min was detected in WYP, WYP-S, WYP-G, and WYP-I. The detailed molecular weights of WYPs are presented in Table 1. Molecular weights of WYP, WYP-S, WYP-G, and WYP-I were measured as 3.344×10^5, 3.338×10^5, 3.205×10^5, and 3.200×10^5 Da, respectively, suggesting that the molecular weight of WYP slightly declined after the *in vitro* simulated digestion. The decline in molecular weight of WYP after the *in vitro* simulated digestion might be owing to the cleavage of the glycosidic linkages in the polymer chains (Huang et al., 2020).

3.1.3. Dynamic variation in C_R

As shown in Table S1 (Supplementary material), the C_R released from WYP after the simulated saliva-digestion ranged from 0.126 ± 0.006 to 0.124 ± 0.012 mg/mL, showing no obvious difference. Conversely, the C_R released from WYP significantly ($p < 0.05$) increased from 0.364 ± 0.112 to 0.684 ± 0.111 mg/mL after the simulated gastric-digestion. Subsequently, the C_R released from WYP was overall stable after the simulated intestinal-digestion, ranging from 0.721 ± 0.066 to 0.828 ± 0.056 mg/mL. These results were similar with the change behaviors of the C_R released from okra pectic-polysaccharides and tea pectic-polysaccharides (Li, Wang, Yuan, Pan, & Chen, 2018; Wu, Nie et al., 2021), which further confirmed that the decline in molecular weight of WYP was owing to the breakdown of glycosidic linkages in the polymer chains. Besides, the change in C_R was also in accordance with the

Table 1
Dynamic variations in digestibility, fermentability, chemical composition, molecular weight (*Mw*), and constituent monosaccharide of WYP during *in vitro* simulated digestion and fermentation by human feces.

	WYP	WYP-S	WYP-G	WYP-I	WYPI-6	WYPI-12	WYPI-24	WYPI-48
Digestibility/ Fermentability (%)	–	1.26	6.92	8.38	8.60	17.26	30.92	42.18
Total polysaccharides (%)	83.49 ± 1.35 ^{a}	83.83 ± 1.14 ^{a}	79.91 ± 1.99^{b}	79.25 ± 1.58^{b}	53.53 ± 2.16^{c}	50.57 ± 2.07 ^{cd}	47.58 ± 1.72 ^{d}	48.31 ± 3.20 ^{d}
Total uronic acids (%)	43.33 ± 1.08 ^{a}	43.39 ± 2.03 ^{a}	45.39 ± 1.05 ^{a}	45.15 ± 2.04 ^{a}	35.06 ± 0.97^{b}	34.32 ± 0.65^{b}	34.62 ± 1.01^{b}	29.35 ± 1.05^{c}
Degree of esterification (%)	32.11 ± 0.53 ^{a}	32.01 ± 0.73 ^{a}	33.52 ± 0.56 ^{a}	31.72 ± 2.07 ^{a}	3.20 ± 0.02^{b}	2.56 ± 0.19^{b}	2.81 ± 0.01^{b}	2.29 ± 0.03^{b}
$M_w \times 10^5$ (Da)	3.344 ± 0.013 ^{a}	3.338 ± 0.013 ^{a}	3.205 ± 0.013^{b}	3.200 ± 0.010^{b}	2.801 ± 0.014^{c}	2.723 ± 0.016 ^{d}	2.645 ± 0.013 ^{e}	2.498 ± 0.015^{f}
Constituent monosaccharide and molar ratios								
Man	0.06	0.06	0.06	0.06	0.15	0.14	0.15	0.15
Rha	0.08	0.08	0.09	0.08	0.18	0.15	0.12	0.12
GlcA	0.04	0.04	0.05	0.04	0.04	0.03	0.01	0.01
GalA	1.00	1.00	1.00	1.00	1.00	1.00	1.00	1.00
Glc	0.12	0.12	0.08	0.09	0.11	0.10	0.10	0.10
Gal	0.34	0.35	0.37	0.36	0.23	0.19	0.16	0.14
Ara	0.31	0.30	0.32	0.32	0.23	0.19	0.18	0.17

Sample codes were the same as in Fig. 1.Values represent mean ± standard deviation, and different superscript lowercase letters indicated significance ($p < 0.05$) in each row; Statistical significances were carried out by ANOVA and Duncan's test.

digestibility of WYP at different digestion stages *in vitro* (Table 1). Overall, these results suggested that WYP was slightly digested after the *in vitro* simulated digestion.

3.1.4. Dynamic variation in constituent monosaccharide

Monosaccharides and molar ratios can influence the physicochemical properties of dietary polysaccharides, and their utilized hierarchy by colonic microbiota (Payling et al., 2020). Therefore, monosaccharide compositions of WYP, WYP-S, WYP-G, and WYP-I were measured, and the results are presented in Fig. 2A and Table 1. GalA, Gal, Ara, Glc, Rha, Man, and GlcA were measured as the main monosaccharides in WYP, in accordance with a previous study (Guo et al., 2021). Additionally, it was found that the kinds of constituent monosaccharides among WYP, WYP-S, WYP-G, and WYP-I were similar. Indeed, as shown in Table 1, the molar ratio of Glc in WYP-G and WYP-I slightly decreased, which might be owing to the Glc on the branched chain hydrolyzed by the low pH in the simulated gastric fluid (Wu, Nie et al., 2021; Wu, Yuan, et al., 2021).

3.1.5. Dynamic variations in FT-IR spectrum and esterification degree (DE)

The FT-IR spectra of WYP, WYP-S, WYP-G, and WYP-I are shown in Fig. 2C. The results showed that the FT-IR spectra among WYP, WYP-S, WYP-G, and WYP-I were almost identical, indicating that the primarily chemical structure of WYP was overall stable after the *in vitro* simulated digestion. Additionally, the typical signals of acidic polysaccharides, including 3423.79 cm^{-1}, 2919.97 cm^{-1}, 1735.38 cm^{-1}, 1630.21 cm^{-1}, 1438.14 cm^{-1}, and 1236.65 cm^{-1}, were found in WYP and its digested samples (Guo et al., 2021; Wu, Feng, et al., 2021; Wu et al., 2022; Wu, Yuan, et al., 2021; Yan et al., 2019). Results further supported that WYP was an acidic polysaccharide, similar with the previous studies (Chen, Qu, et al., 2009; Chen, Wang, et al., 2009; Wang et al., 2012). Furthermore, the DE value of WYP was also evaluated based on the intensities of 1735.38 cm^{-1} and 1630.21 cm^{-1} signals. The DE values of WYP, WYP-S, WYP-G, and WYP-I were similar, which ranged from 31.72% to 33.52%.

In conclusion, all abovementioned results indicated that WYP was slightly degraded, and the digestibility of WYP was only about 8.38% after the *in vitro* simulated digestion. More than 90% of WYP was the indigestible polysaccharide, which was further applied for *in vitro* fermentation by human feces.

3.2. Dynamic variations in physicochemical characteristics of the indigestible WYP (WYP-I) during in vitro fermentation by human feces

3.2.1. Dynamic variations in fermentability and chemical composition

Table 1 also shows the dynamic variations in fermentability, polysaccharides, and uronic acids of WYP-I at different fermented stages *in vitro*. The contents of total polysaccharides in WYP-I, WYPI-6, WYPI-12, WYPI-24, and WYPI-48 significantly ($p < 0.05$) decreased from 79.25% to 48.31%. The obvious decline of total polysaccharides might be due to the fact that the colonic microbiota could secret carbohydrate active enzymes to destroy the glycosidic bonds of polysaccharides and utilize the degraded fragments, resulting in the decrease of total

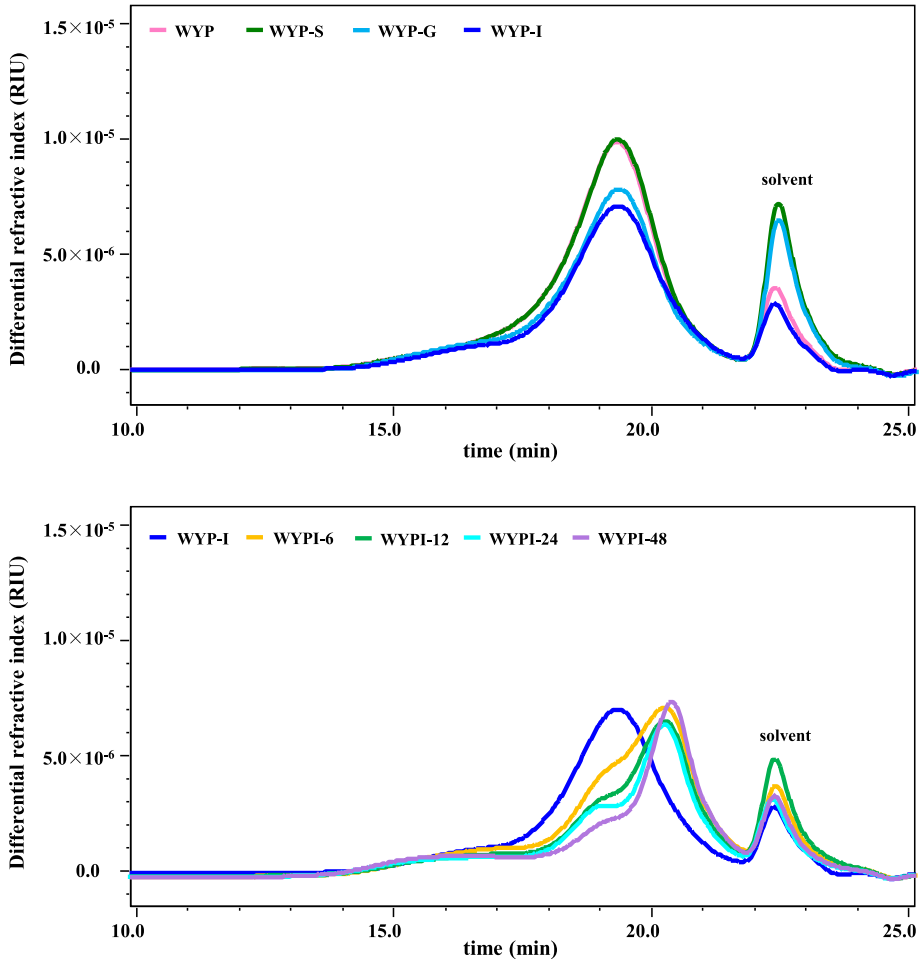

Fig. 1. Dynamic variations in *SEC* profiles of WYP during *in vitro* simulated digestion and fermentation by human feces **WYP**, polysaccharides extracted from 'Wuyi rock' tea; **WYP-S**, **WYP-G**, and **WYP-I**, WYP digested at different digestion stages, including salivary, saliva-gastric, and saliva-gastrointestinal digestions, respectively; **WYPI-6**, **WYPI-12**, **WYPI-24**, and **WYPI-48**, WYP-I fermented by human feces at the time points of 6, 12, 24, and 48 h, respectively.

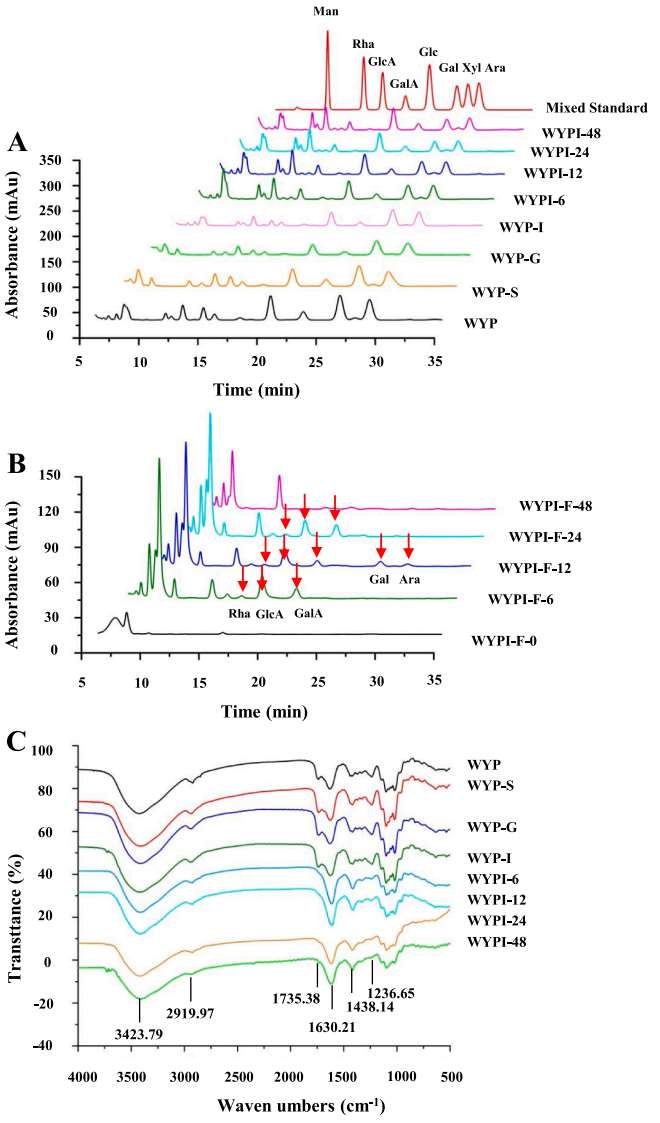

Fig. 2. Dynamic variations in constituent monosaccharides (A), free monosaccharides released (B), and FT-IR spectra (C) of WYP during *in vitro* simulated digestion and fermentation by human feces Sample codes were the same as in Fig. 1; **Man**, mannose; **Rha**, rhamnose; **GlcA**, glucuronic acid; **GalA**, galacturonic acid; **Glc**, glucose; **Gal**, galactose; **Xyl**, xylose; **Ara**, arabinose.

polysaccharides (Huang et al., 2020). The contents of uronic acids in WYP-I, WYPI-6, WYPI-12, WYPI-24, and WYPI-48 also significantly ($p < 0.05$) decreased from 45.15% to 29.35%. The decline of uronic acids might be owing to the hydrolysis of GlcA and GalA in WYP-I, which could be degraded by certain intestinal microbes (Ding et al., 2019). In addition, the fermentability of WYP-I at different fermented time points obviously enhanced from 8.60% to 42.18%. The results showed that WYP-I could be well utilized by colonic microbiota in human feces (Kong et al., 2021).

3.2.2. Dynamic variations in C_R and free monosaccharides

Previous studies have shown that the colonic microbiota can break down dietary polysaccharides, and then reducing sugars are produced to be utilized by intestinal microbiota in turn (Wu, Fu, et al., 2021; Wu, Yuan, et al., 2021). The dynamic variation in C_R released from WYP-I during the fermentation process is also shown in Table S1. The C_R significantly raised to the high content (1.111 ± 0.027 mg/mL) at the fermentation time point of 12 h, and then declined to the low content (0.602 ± 0.041 mg/mL) at the fermentation time point of 48 h, which was similar with a previous result (Zhou, Zhang, Huang, Yang, & Huang, 2020). Results revealed that the release rate of reducing sugars was faster than its consumption rate before the *in vitro* fermentation time point of 12 h, while its consumption rate was faster than the release rate with the increasing time from 12 h to 48 h (Kong et al., 2021).

Furthermore, as shown in Fig. 2B, the free sugars released from WYP-I after the *in vitro* fermentation by human feces were further analyzed by HPLC. The observed free sugars indicated that the indigestible WYP (WYP-I) could be degraded by colonic microbiota in human feces. A previous study has demonstrated that some bacteria, such as *Bacteroides thetaiotaomicron* and *Bacteroides ovatus*, can metabolize certain glycans (Koropatkin, Cameron, & Martens, 2012; Ndeh et al., 2017). After the *in vitro* fermentation for 6 h, three types of free sugars, including Rha, GlcA, and GalA, were detected in the fermented mixture. Indeed, five types of free sugars, including Rha, GlcA, GalA, Gal, and Ara, were detected in the fermented mixture at the fermentation time point of 12 h. Furthermore, the responses of free sugars gradually declined with the increasing time from 12 h to 48 h. The dynamic change behavior of free sugars was similar with that of reducing sugar contents, suggesting that WYP-I was utilized by colonic microbiota in human feces during *in vitro* fermentation.

3.2.3. Dynamic variations in molecular weight, constituent monosaccharide, and FT-IR spectrum

As shown in Fig. 1, the *SEC* profile of the indigestible WYP (WYP-I) gradually shifted to the right with the increase of retention time, further confirming that WYP-I was utilized by intestinal microbiota. The molecular weight of WYP-I remarkably declined from 3.200×10^5 to 2.498×10^5 Da after the *in vitro* fermentation, indicating that WYP-I was degraded into relatively small fragments and further utilized by intestinal microbes (Wu, Nie et al., 2021). Taken together with the results of C_R and free monosaccharides, it could be presumed that the dynamic decline of molecular weight of WYP-I at different fermentation time points might be primarily due to the breakdown of its glycosidic linkages. Previous results also showed that molecular weights of acidic polysaccharides from *Abelmoschus esculentus*, chrysanthemum tea, and loquat leaf obviously declined after the *in vitro* fermentation by human feces (Wu, Nie et al., 2021; Wu, Fu, et al., 2021; Wu, Yuan, et al., 2021).

Generally, the colonic microbiota could change the molar ratio of monosaccharides in dietary polysaccharides during *in vitro* fermentation (Ding et al., 2019). As shown in Fig. 2A and Table 1, Man, Rha, GlcA, GalA, Glc, Gal, and Ara were also measured as the main constituent monosaccharides in WYP-I, WYPI-6, WYPI-12, WYPI-24, and WYPI-48. Results showed that the *in vitro* fermentation by human feces obviously affected their molar ratio, but had no effects on the types. At the fermented time point of 48 h, the molar ratio of GlcA, Gal, and Ara decreased, suggesting that WYP-I was utilized by colonic microbiota in human feces. Taken together with the results of total uronic acids (Table 1) and free monosaccharides (Fig. 2B), results indicated that pectic-polysaccharides and arabinogalactan in WYP-I could be hydrolyzed and used by colonic microbes (Wu, Fu, et al., 2021). Generally, pectic-polysaccharides can be easily hydrolyzed and used by *Bacteroides* and *Bifidobacteria* (Ndeh et al., 2017). Moreover, arabinogalactan can also be degraded and utilized by *Bifidobacteria* (Wu, Yuan, et al., 2021).

Furthermore, as shown in Fig. 2C, the signals of 3423.79 cm^{-1}, 2919.97 cm^{-1}, 1735.38 cm^{-1}, 1630.21 cm^{-1}, 1438.14 cm^{-1}, and 1236.65 cm^{-1}, which existed in WYP and WYP-I, were also found in WYPI-6, WYPI-12, WYPI-24, and WYPI-48. However, the intensity of 1735.38 cm^{-1} signal in fermented samples obviously declined when compared with WYP-I. Indeed, as shown in Table 1, the DE values of fermented samples were remarkably lower than that of WYP and WYP-I, which was similar to a formerly reported result (Wu, Yuan, et al., 2021). The DE value of pectic-polysaccharides could be altered during *in vitro* fermentation by human feces.

3.3. Effects of the indigestible WYP (WYP-I) on pH values and SCFAs production during in vitro fermentation by human feces

Generally, the dynamic variation in pH values of the fermented mixture during the *in vitro* fermentation by human feces could indirectly reflect the degradation and utilization of natural polysaccharides by colonic microbiota. The dynamic variation in pH values after different time points of fermentation is listed in Table 2. The initial pH values among the BLANK, INULIN, and WYPI groups were similar. However, after the *in vitro* fermentation at different time points, the pH values of WYPI and INULIN groups were lower than that of the negative control group, indicating that the addition of WYP-I and inulin had an obvious influence on the pH during *in vitro* fermentation by human feces. Previous studies showed that the generation of SCFAs could lower the pH of their surroundings (Kong et al., 2021).

SCFAs, the important metabolites of dietary polysaccharides produced by colonic microbiota during *in vitro* fermentation, play essential roles in keeping the barrier function of intestine, modulating the epithelial proliferation, inhibiting colorectal cancers, and regulating immune responses (Zhang et al., 2020). Consequently, the measurement of SCFAs is essential when evaluating the fermentation properties of dietary polysaccharides. The concentrations of total SCFAs and individual SCFA, including acetic, propionic, *i*-butyric, *n*-butyric, *i*-valeric, and *n*-valeric acids produced in the BLANK, INULIN, and WYPI groups, are shown in Table 2. An increase of the levels of total SCFAs was found in three groups after the *in vitro* fermentation for 48 h. In the experimental (WYPI) group, the concentration of total SCFAs reached 16.50 ± 0.19 mmol/L after the *in vitro* fermentation by human feces for 48 h, which was higher than that of the negative control group (10.81 ± 0.13 mmol/L), and was close to the positive control group (16.75 ± 0.06 mmol/L). Indeed, the dominant SCFAs in three groups were detected as acetic, propionic, *n*-butyric, and *n*-valeric acids. Meanwhile, the acetic acid in the WYPI group after the *in vitro* fermentation by human feces for 48 h was 9.65 ± 0.23 mmol/L, which was also significantly higher than that of the negative control group (6.82 ± 0.01 mmol/L). Acetate, the fermentation metabolite of *Bifidobacterium*, is the most abundant SCFA in peripheral circulation, which can utilized in brain, heart, and peripheral tissues (Liu et al., 2021; Zhang et al., 2020). Indeed, acetate is able to cross the blood–brain barrier to reduce appetite *via* a central homeostatic mechanism (Wu, Nie et al., 2021). The propionic acid in the WYPI group (3.36 ± 0.09 mmol/L) after *in vitro* fermentation for 48 h was also higher than that of the negative control group (1.50 ± 0.05 mmol/L). Usually, propionic acid can decrease the level of fatty acid, reduce food intake, and improve the sensitivity of tissue insulin (Ding et al., 2019), which could be generated by *Phascolarctobacterium* (Ding et al., 2019). Besides, after the *in vitro* fermentation by human feces for 48 h, the concentrations of *n*-butyric and *n*-valeric acids in the WYPI group were determined to be 1.11 ± 0.16 mmol/L and 1.53 ± 0.07 mmol/L, respectively, which also higher than that of the negative control group. Butyric acid plays an important role in maintaining the integrity of colonic epithelium and regulating the expression of tight junction proteins and related genes (Han et al., 2020). In conclusion, results indicated that WYP possessed a potential prebiotic effect *via* increasing the generation of SCFAs.

3.4. Effect of the indigestible WYP (WYP-I) on the modulation of gut microbial composition

Intestinal microbiota plays an essential role in the host, including providing the host with nutrients, defending against invading pathogens, and maintaining intestinal homeostasis (Zhang, Liu, Chen, Aweya, & Cheong, 2020). A previous study showed that tea pectic-polysaccharides could be hydrolyzed and used by colonic bacteria, resulting in modulation of the microbial composition and abundance (Chen et al., 2018). Thus, it is quite necessary to understand the relationships among polysaccharides from Wuyi rock tea, colonic microbiota, and microbial metabolites, which can be beneficial to promoting intestinal health by regulating the intestinal bacteria.

In the current study, the high-throughput sequencing analysis was performed on samples from the BLANK, INULIN, and WYPI groups after the *in vitro* fermentation by human feces for 48 h to reveal the effect of the indigestible WYP on the modulation of gut microbial composition. The rarefaction curves, the Shannon indexes, and principal component analysis (PCA) are shown in Fig. S1 (Supplementary material). Rarefaction curves showed that the richness of bacterial species appeared to be stable as the number of sequences samples increased, indicating that sample sequences were sufficient. Besides, the saturation of the Shannon indexes indicated that the sequencing data was large enough to cover all the bacteria species. Further, PCA was used to reveal a distinct clustering of microbial compositions from different samples. Results clearly showed that each group was obviously different from others (Figure S1). Overall, results demonstrated that the microbial composition in the WYPI group was notably different from that in the negative control group.

Table 2
Dynamic variations in pH values and contents of short-chain fatty acids produced at different time points of fermentation.

			Short-chain fatty acids (mmol/L)						
Groups	Time (h)	pH value	Acetic acid	Propionic acid	*i*-Butyric acid	*n*-Butyric acid	*i*-Valeric acid	*n*-Valeric acid	Total
BLANK	0	8.96 ± 0.01	ND	ND	ND	ND	ND	ND	ND
	6	8.74 ± 0.02	$5.23 \pm 0.10^{b, C}$	ND	ND	ND	ND	ND	$5.23 \pm 0.10^{b, C}$
	12	8.58 ± 0.02	$6.04 \pm 0.09^{b, B}$	$1.52 \pm 0.01^{a, A}$	$0.30 \pm 0.06^{a, A}$	$0.70 \pm 0.02^{a, B}$	$0.41 \pm 0.14^{a, A}$	$0.78 \pm 0.04^{c, B}$	$9.75 \pm 0.21^{b, B}$
	24	8.13 ± 0.02	$6.64 \pm 0.04^{b, A}$	$1.69 \pm 0.11^{b, A}$	$0.29 \pm 0.05^{b, A}$	$0.80 \pm 0.01^{c, AB}$	$0.56 \pm 0.01^{a, A}$	$0.86 \pm 0.05^{a, AB}$	$10.84 \pm 0.27^{b, A}$
	48	7.91 ± 0.02	$6.82 \pm 0.01^{b, A}$	$1.50 \pm 0.05^{c, A}$	$0.36 \pm 0.01^{b, A}$	$0.90 \pm 0.10^{a, A}$	$0.29 \pm 0.07^{a, A}$	$0.94 \pm 0.02^{b, A}$	$10.81 \pm 0.13^{b, A}$
INULIN	0	9.10 ± 0.03	ND	ND	ND	ND	ND	ND	ND
	6	7.39 ± 0.04	$6.24 \pm 0.06^{a, D}$	$1.73 \pm 0.03^{a, B}$	$0.28 \pm 0.03^{b, C}$	$0.82 \pm 0.03^{b, A}$	$0.38 \pm 0.02^{ab, A}$	$1.25 \pm 0.02^{a, A}$	$10.70 \pm 0.03^{a, D}$
	12	6.73 ± 0.03	$7.19 \pm 0.17^{a, C}$	$1.65 \pm 0.13^{a, B}$	$0.38 \pm 0.02^{a, B}$	$0.76 \pm 0.10^{a, A}$	$0.36 \pm 0.04^{a, A}$	$1.19 \pm 0.08^{b, A}$	$11.52 \pm 0.08^{a, C}$
	24	5.81 ± 0.02	$8.24 \pm 0.01^{a, B}$	$1.81 \pm 0.01^{b, B}$	$0.42 \pm 0.01^{ab, B}$	$0.84 \pm 0.01^{b, A}$	$0.31 \pm 0.05^{b, A}$	$1.06 \pm 0.03^{a, B}$	$12.69 \pm 0.06^{a, B}$
	48	5.15 ± 0.03	$9.72 \pm 0.01^{a, A}$	$3.56 \pm 0.03^{a, A}$	$1.24 \pm 0.02^{a, A}$	$0.79 \pm 0.03^{a, A}$	$0.39 \pm 0.04^{a, A}$	$1.05 \pm 0.03^{b, B}$	$16.75 \pm 0.06^{a, A}$
WYPI	0	8.71 ± 0.01	ND	ND	ND	ND	ND	ND	ND
	6	7.10 ± 0.02	$6.13 \pm 0.22^{a, C}$	$1.83 \pm 0.53^{a, B}$	$0.40 \pm 0.05^{a, AB}$	$0.94 \pm 0.01^{a, AB}$	$0.49 \pm 0.23^{a, A}$	$1.10 \pm 0.10^{a, B}$	$10.89 \pm 0.35^{a, D}$
	12	6.52 ± 0.01	$6.42 \pm 0.57^{ab, C}$	$1.79 \pm 0.26^{a, B}$	$0.34 \pm 0.01^{a, B}$	$0.86 \pm 0.02^{a, B}$	$0.37 \pm 0.02^{a, A}$	$2.03 \pm 0.20^{a, A}$	$11.82 \pm 0.10^{a, C}$
	24	5.41 ± 0.01	$7.76 \pm 0.27^{a, B}$	$2.33 \pm 0.02^{a, B}$	$0.55 \pm 0.10^{a, A}$	$1.02 \pm 0.01^{a, AB}$	$0.38 \pm 0.11^{ab, A}$	$1.65 \pm 0.54^{a, AB}$	$13.68 \pm 0.49^{a, B}$
	48	5.12 ± 0.01	$9.65 \pm 0.23^{a, A}$	$3.36 \pm 0.09^{b, A}$	$0.41 \pm 0.07^{b, AB}$	$1.11 \pm 0.16^{a, A}$	$0.44 \pm 0.04^{a, A}$	$1.53 \pm 0.07^{a, AB}$	$16.50 \pm 0.19^{a, A}$

Sample codes were the same as in Fig. 3. Values represent mean ± standard deviation, and different superscript letters showed significant differences among different time ($p < 0.05$) in the same group, while minuscules represented significant differences among different groups ($p < 0.05$) at the same time point; ND: not detected.

The changes in microbial compositions in different groups are exhibited in Fig. 3. At the phylum level (Fig. 3A), the major microbes in the negative control group (BLANK) were identified as *Proteobacteria* (38.42%), *Fusobacteria* (34.38%), *Firmicutes* (15.08%), *Bacteroidetes* (10.65%), and *Actinobacteria* (1.42%). The WYPI group showed remarkable increases in the relative abundances of *Bacteroidetes* (35.25%) and *Firmicutes* (30.76%) compared with the negative control group. *Bacteroidetes* can hydrolyze the indigestible polysaccharide to generate SCFAs by encoding various carbohydrate active enzymes, such as glycosidase and polysaccharide lyase (Liu et al., 2021). The WYP-I could up-regulate the ratio of *Bacteroidetes/ Firmicutes* from 0.71 (BLANK group) to 1.15 (WYPI group). It has been reported that the increase of the ratio of *Bacteroidetes/ Firmicutes* can lead to the decline of the energy harvest, which is positively correlated to a reduced risk of obesity in human (Chen et al., 2018). Thus, WYP is expected to be developed as a functional food for reducing obesity. The WYPI group also showed remarkable decreases in the relative abundances of *Fusobacteria* (0.53%) and *Proteobacteria* (27.37%) compared with the BLANK group. Previous studies showed that *Fusobacteria* might be closely correlated to the gastric oncogenesis, and *Proteobacteria* might be associated with the chronic colitis (Wu, Fu, et al., 2021). In addition, the abundances of *Actinobacteria* also increased in the WYPI group (5.98%) and the INULIN group (4.12%) compared with that of the BLANK group (1.42%). *Bifidobacterium*, the representative of *Actinobacteria,* is an essential probiotic in the colon for human intestinal health, which can control serum cholesterol levels, prevent intestinal diseases, modulate immune system, and possess anti-cancer activities (Wu, Nie et al., 2021). Furthermore, the relative abundance of *Bacteroidetes* (9.41%) and *Firmicutes* (15.96%) in the INULIN group was close to that of the BLANK group. The relative abundance of *Fusobacteria* (0.42%) decreased, while that of *Proteobacteria* (70.06%) increased. This result might be owing to the fact that *Escherichia-Shigella* likely utilized low molar mass carbon sources to maintain its growth (Zhang et al., 2020). These results indicated that WYP-I could obviously regulate the microbial composition *via*

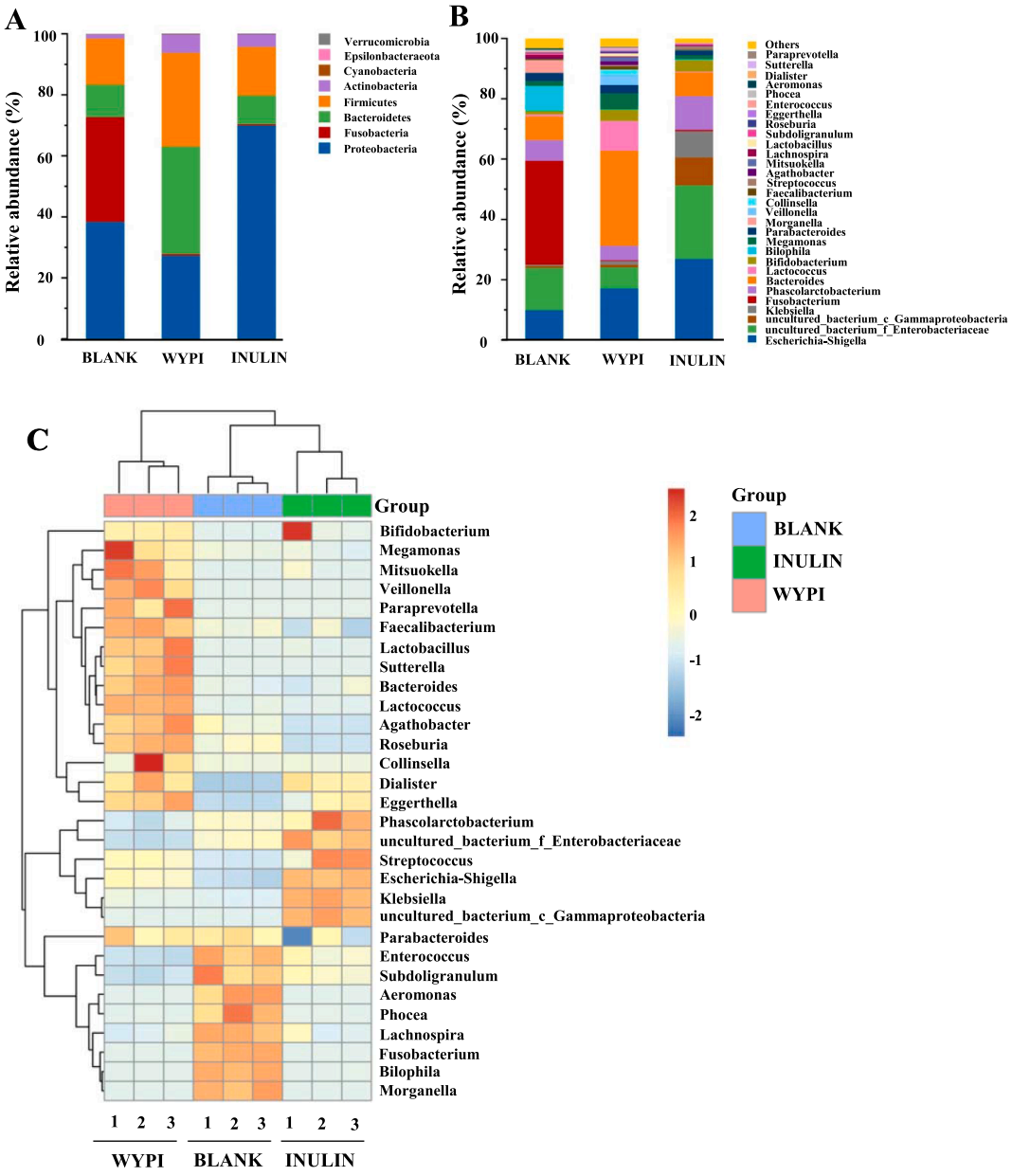

Fig. 3. The relative abundance of bacterial community at the phylum level (A) and the genus level (B), and the heatmap analysis of the relative abundance of bacterial community at the genus level (C) **BLANK,** the blank control (no additional carbon source supplement); **INULIN,** the positive control (INULIN supplement); **WYPI,** the experimental group (WYP-I supplement).

up-regulating the proliferation of beneficial bacteria and down-regulating the proliferation of harmful bacteria.

At the genus level (Fig. 3B), the negative control group was mainly consisted of *Fusobacterium* (34.38%), *uncultured_bacterium_f_Enterobacteriaceae* (14.01%), *Escherichia-Shigella* (10.02%), *Bilophila* (8.18%), and *Bacteroides* (7.82%). The WYPI group caused a notable increase in the relative abundance of *Bacteroides* (31.55%). *Bacteroides* could hydrolyze and use pectic-polysaccharides in the WYPI group to keep its growth, and prevent the host against colorectal cancer and inflammation, as well as improve metabolic disorders in obese individuals (Ding et al., 2019). The WYPI group also exhibited higher levels of *Lactococcus* (9.82%) and *Bifidobacterium* (3.76%) than that of the BLANK group. *Lactococcus* has been proved to be a kind of potential probiotic bacteria (Liu et al., 2021). *Bifidobacterium*, regarded as health-promoting gut microbiota, can produce α-glucosidases, β-galactosidases, and other enzymes to hydrolyze carbohydrates (Han et al., 2020). The WYPI group exhibited a lower level of *Phascolarctobacterium* (4.79%) than that of the BLANK group, which was found to be a substantial acetate/propionate-producer (Yuan, Li, You, Dong, & Fu, 2020). Furthermore, the relative abundances of harmful intestinal bacteria in the WYPI group (26.68%), such as *Fusobacterium*, *Bilophila*, *Escherichia-Shigella*, *uncultured_bacterium_f_Enterobacteriaceae*, *uncultured_bacterium_c_Gammaproteobacteria*, and *Klebsiella*, remarkably decreased when compared with the negative control group (67.74%). *Fusobacterium* might be related to gastric oncogenesis (Han et al., 2020). Besides, the increase of *Bifidobacterium* (3.88%) and *Phascolarctobacterium* (11.19%) was observed in the INULIN group, but the total level of harmful intestinal bacteria (70.04%) increased.

The heat map in Fig. 3C indicates the relative abundances of top 30 bacteria at the genus level in the BLANK, WYPI, and INULIN groups. An increase of the relative abundances of the beneficial bacteria genus, such as *Megamonas*, *Veillonella*, *Faecalibacterium*, *Lactobacillus*, *Bifidobacterium*, *Bacteroides*, *Lactococcus*, *Agathobacter*, *Roseburia*, *Collinsella*, *Dialister*, and *Eggerthella,* was found in the WYPI group, while an increase of abundances of the beneficial bacteria genus, such as *Phascolarctobacterium* and *Bifidobacterium,* was found in the INULIN group. These results indicated that the microbial composition was shaped by the WYP-I and INULIN supplementation.

The results of LEfSe are exhibited in Figure 4. As shown in Figure 4A, a total of 25 genera, whose LDA scores were above 4.0, showed obvious

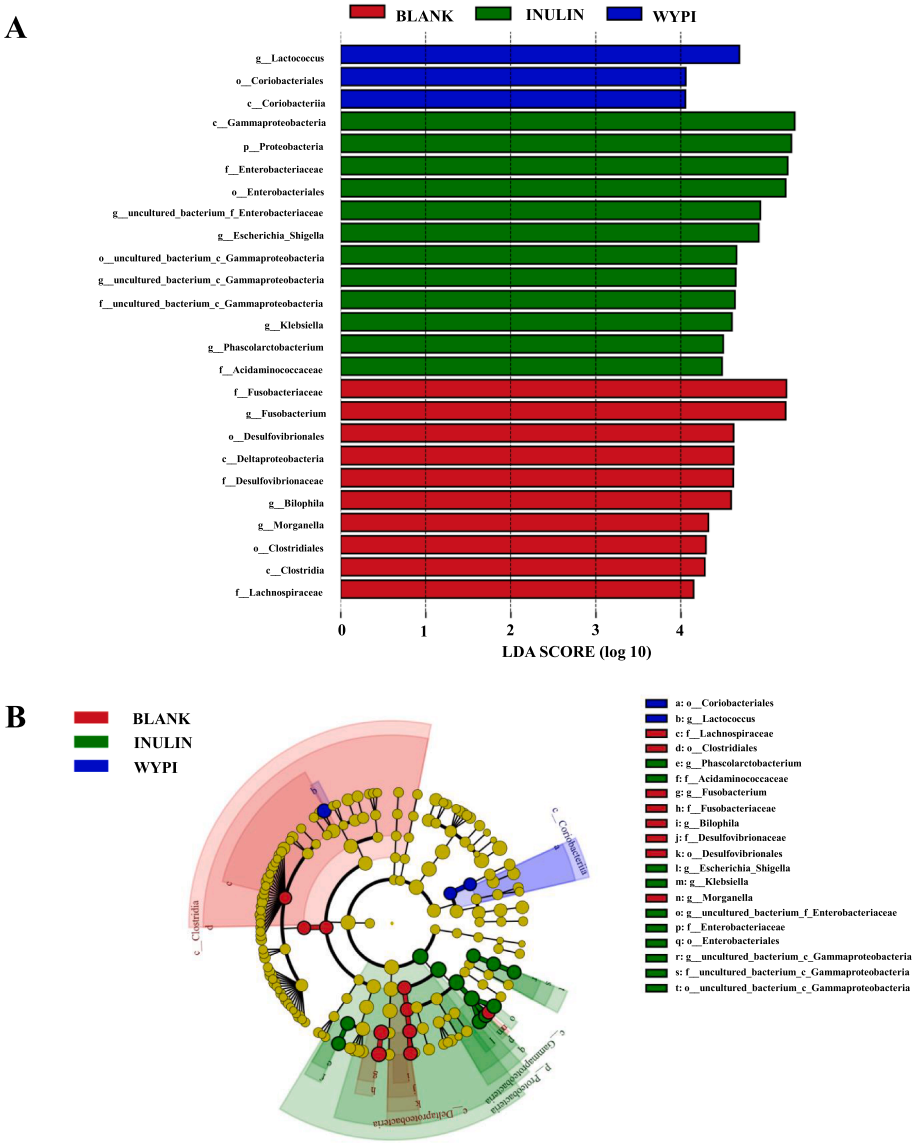

Fig. 4. Linear discriminant analysis (LDA) score for taxa differing (A) and LEfSe evolutionary branch graph (B) between the BLANK, INULIN, and WYPI groups Sample codes were the same as in Fig. 3.

differences among all groups. There were 3, 12, and 10 kinds of dominant genera in WYPI, INULIN, and BLANK groups, respectively. As shown in Fig. 4B, there were 2, 8, and 10 kinds of dominant statistically significant species in WYPI (color in blue), BLANK (color in red), and INULIN (color in green) groups, respectively. Especially, *Lactococcus* was found in WYPI group as the dominant species, which indicated that the supplement of WYP-I could notably change the microbial composition.

4. Conclusion

In this study, WYP was degraded slightly, and the digestibility of WYP was only about 8.38% after *in vitro* simulated digestion. Physicochemical properties of WYP, including molecular weight, compositional monosaccharide, chemical composition, also changed slightly under the simulated digestion conditions. Furthermore, the colonic microbiota in human feces could degrade and utilize the indigestible WYP during the *in vitro* fermentation, resulting in the modulation of its composition and abundance. Notably, WYP-I could stimulate the proliferation of several beneficial bacteria, such as *Bacteroides*, *Lactococcus*, and *Bifidobacterium*, and promote the generation of SCFAs. The findings from the present study are beneficial to revealing the potential digestive and fermented characteristics of WYP, and WYP can be developed and utilized as a prebiotic supplement to improve gut health.

Declaration of Competing Interest

The authors declare that they have no known competing financial interests or personal relationships that could have appeared to influence the work reported in this paper.

Acknowledgements

This work was supported by the Scientific Research Foundation of Chengdu University (No. 2081921047), the opening fund of the State Key Laboratory of Quality Research in Chinese Medicine, University of Macau (No. QRCM-OP21001), and the opening fund of the Key Laboratory of Coarse Cereal Processing, Ministry of Agriculture and Rural Affairs, Chengdu University (No. 2021CC002).

Appendix A. Supplementary data

Supplementary data to this article can be found online at https://doi.org/10.1016/j.fochx.2022.100288.

References

Brodkorb, A., Egger, L., Alminger, M., Alvito, P., Assuncao, R., Ballance, S., … Recio, I. (2019). INFOGEST static *in vitro* simulation of gastrointestinal food digestion. *Nature Protocols, 14*(4), 991–1014.

Chen, H. X., Qu, Z., Fu, L. L., Dong, P., & Zhang, X. (2009). Physicochemical properties and antioxidant capacity of 3 polysaccharides from green tea, oolong tea, and black tea. *Journal of Food Science, 74*(6), C469–C474.

Chen, H. X., Wang, Z. S., Qu, Z. S., Fu, L. L., Dong, P., & Zhang, X. (2009). Physicochemical characterization and antioxidant activity of a polysaccharide isolated from oolong tea. *European Food Research and Technology, 229*(4), 629–635.

Chen, G., Xie, M., Wan, P., Chen, D., Ye, H., Chen, L., … Liu, Z. (2018). Digestion under saliva, simulated gastric and small intestinal conditions and fermentation *in vitro* by human intestinal microbiota of polysaccharides from Fuzhuan brick tea. *Food Chemistry, 244*, 331–339.

Chen, G. J., Yuan, Q. X., Saeeduddin, M., Ou, S. Y., Zeng, X. X., & Ye, H. (2016). Recent advances in tea polysaccharides: Extraction, purification, physicochemical characterization and bioactivities. *Carbohydrate Polymers, 153*, 663–678.

Ding, Y., Yan, Y., Peng, Y., Chen, D., Mi, J., Lu, L., … Cao, Y. (2019). *In vitro* digestion under simulated saliva, gastric and small intestinal conditions and fermentation by human gut microbiota of polysaccharides from the fruits of *Lycium barbarum*. *International Journal of Biological Macromolecules, 125*, 751–760.

Guo, Y., Chen, X., Gong, P., Chen, F., Cui, D., & Wang, M. (2021). Advances in the *in vitro* digestion and fermentation of polysaccharides. *International Journal of Food Science & Technology, 56*(10), 4970–4982.

Guo, H., Fu, M. X., Wu, D. T., Zhao, Y. X., Li, H., Li, H. B., & Gan, R. Y. (2021). Structural characteristics of crude polysaccharides from 12 selected Chinese teas, and their antioxidant and anti-diabetic activities. *Antioxidants, 10*(10), 1562.

Guo, X., Ho, C.-T., Wan, X., Zhu, H., Liu, Q., & Wen, Z. (2021). Changes of volatile compounds and odor profiles in Wuyi rock tea during processing. *Food Chemistry, 341*(Part 1), Article 128230.

Han, R., Pang, D., Wen, L., You, L., Huang, R., & Kulikouskaya, V. (2020). *In vitro* digestibility and prebiotic activities of a sulfated polysaccharide from *Gracilaria Lemaneiformis*. *Journal of Functional Foods, 64*, Article 103652.

Huang, F., Hong, R., Yi, Y., Bai, Y., Dong, L., Jia, X., … Wu, J. (2020). *In vitro* digestion and human gut microbiota fermentation of longan pulp polysaccharides as affected by *Lactobacillus fermentum* fermentation. *International Journal of Biological Macromolecules, 147*, 363–368.

Jiang, H., Yu, F., Qin, L., Zhang, N., Cao, Q., Schwab, W., … Song, C. (2019). Dynamic change in amino acids, catechins, alkaloids, and gallic acid in six types of tea processed from the same batch of fresh tea (*Camellia sinensis* L.) leaves. *Journal of Food Composition and Analysis, 77*, 28–38.

Kong, Q., Zhang, R., You, L., Ma, Y., Liao, L., & Pedisić, S. (2021). *In vitro* fermentation characteristics of polysaccharide from Sargassum fusiforme and its modulation effects on gut microbiota. *Food and Chemical Toxicology, 151*, Article 112145.

Koropatkin, N. M., Cameron, E. A., & Martens, E. C. (2012). How glycan metabolism shapes the human gut microbiota. *Nature Reviews Microbiology, 10*(5), 323–335.

Li, J., Pang, B., Yan, X., Shang, X., Hu, X., & Shi, J. (2020). Prebiotic properties of different polysaccharide fractions from *Artemisia sphaerocephala* Krasch seeds evaluated by simulated digestion and *in vitro* fermentation by human fecal microbiota. *International Journal of Biological Macromolecules, 162*, 414–424.

Li, W. W., Wang, C., Yuan, G. Q., Pan, Y. X., & Chen, H. X. (2018). Physicochemical characterisation and α-amylase inhibitory activity of tea polysaccharides under simulated salivary, gastric and intestinal conditions. *International Journal of Food Science and Technology, 53*(2), 423–429.

Li, C., Yu, W. W., Wu, P., & Chen, X. D. (2020). Current *in vitro* digestion systems for understanding food digestion in human upper gastrointestinal tract. *Trends in Food Science & Technology, 96*, 114–126.

Liu, Z. B., Chen, F. C., Sun, J. Y., & Ni, L. (2022). Dynamic changes of volatile and phenolic components during the whole manufacturing process of Wuyi Rock tea (Rougui). *Food Chemistry, 367*, Article 130624.

Liu, C., Du, P., Cheng, Y., Guo, Y., Hu, B., Yao, W., … Qian, H. (2021). Study on fecal fermentation characteristics of aloe polysaccharides *in vitro* and their predictive modeling. *Carbohydrate Polymers, 256*, Article 117571.

Liu, W., Li, Z., Yang, K., Sun, P., & Cai, M. (2021). Effect of nanoemulsion loading finger citron (*Citrus medica* L. var. Sarcodactylis) essential oil on human gut microbiota. *Journal of Functional Foods, 77*, Article 104336.

Ndeh, D., Rogowski, A., Cartmell, A., Luis, A. S., Basle, A., Gray, J., … Gilbert, H. J. (2017). Complex pectin metabolism by gut bacteria reveals novel catalytic functions. *Nature, 544*, 65–70.

Payling, L., Fraser, K., Loveday, S. M., Sims, I., Roy, N., & McNabb, W. (2020). The effects of carbohydrate structure on the composition and functionality of the human gut microbiota. *Trends in Food Science & Technology, 97*, 233–248.

Rui, Y., Wan, P., Chen, G. J., Xie, M. H., Sun, Y., Zeng, X. X., & Liu, Z. H. (2019). Simulated digestion and fermentation *in vitro* by human gut microbiota of intra- and extra-cellular polysaccharides from *Aspergillus cristatus*. *LWT-Food Science and Technology, 116*, 167–174.

Wang, L., Li, C., Huang, Q., Fu, X., & Liu, R. H. (2019). *In vitro* digestibility and prebiotic potential of a novel polysaccharide from *Rosa roxburghii* Tratt fruit. *Journal of Functional Foods, 52*, 408–417.

Wang, Y., Shao, S., Xu, P., Chen, H., Lin-Shiau, S.-Y., Deng, Y.-T., & Lin, J.-K. (2012). Fermentation process enhanced production and bioactivities of oolong tea polysaccharides. *Food Research International, 46*(1), 158–166.

Wu, D. T., Feng, K. L., Huang, L., Gan, R. Y., Hu, Y. C., & Zou, L. (2021). Deep eutectic solvent-assisted extraction, partially structural characterization, and bioactivities of acidic polysaccharides from lotus leaves. *Foods, 10*, 2330.

Wu, D. T., Fu, Y., Guo, H., Yuan, Q., Nie, X. R., Wang, S. P., & Gan, R. Y. (2021). *In vitro* simulated digestion and fecal fermentation of polysaccharides from loquat leaves: Dynamic changes in physicochemical properties and impacts on human gut microbiota. *International Journal of Biological Macromolecules, 168*, 733–742.

Wu, D. T., He, Y., Fu, M. X., Gan, R. Y., Hu, Y. C., Peng, L. X., … Zou, L. (2022). Structural characteristics and biological activities of a pectic-polysaccharide from okra affected by ultrasound assisted metal-free Fenton reaction. *Food Hydrocolloids, 122*, Article 107085.

Wu, D. T., He, Y., Fu, M. X., Gan, R. Y., Hu, Y. C., & Zou, L. (2021). Changes in physicochemical and biological properties of polyphenolic-protein-polysaccharide ternary complexes from *Hovenia dulcis* after in vitro simulated saliva-gastrointestinal digestion. *Foods, 10*, 2322.

Wu, D.-T., Nie, X.-R., Gan, R.-Y., Guo, H., Fu, Y., Yuan, Q., … Qin, W. (2021). *In vitro* digestion and fecal fermentation behaviors of a pectic polysaccharide from okra (*Abelmoschus esculentus*) and its impacts on human gut microbiota. *Food Hydrocolloids, 114*, Article 106577.

Wu, D. T., Yuan, Q., Guo, H., Fu, Y., Li, F., Wang, S. P., & Gan, R. Y. (2021). Dynamic changes of structural characteristics of snow chrysanthemum polysaccharides during *in vitro* digestion and fecal fermentation and related impacts on gut microbiota. *Food Research International, 141*, Article 109888.

Xu, L. L., Chen, Y., Chen, Z. Q., Gao, X. D., Wang, C. L., Panichayupakaranant, P., & Chen, H. X. (2020). Ultrafiltration isolation, physicochemical characterization, and antidiabetic activities analysis of polysaccharides from green tea, oolong tea, and black tea. *Journal of Food Science, 85*(11), 4025–4032.

Xu, A. N., Lai, W. Y., Chen, P., Awasthi, M. K., Chen, X. Q., Wang, Y. F., & Xu, P. (2021). A comprehensive review on polysaccharide conjugates derived from tea leaves: Composition, structure, function and application. *Trends in Food Science & Technology, 114*, 83–99.

Yan, J., Zhou, B., Xi, Y., Huan, H., Li, M., Yu, J., … Shi, Z. (2019). Fermented feed regulates growth performance and the cecal microbiota community in geese. *Poultry Science, 98*(10), 4673–4684.

Yuan, D., Li, C., You, L., Dong, H., & Fu, X. (2020). Changes of digestive and fermentation properties of *Sargassum pallidum* polysaccharide after ultrasonic degradation and its impacts on gut microbiota. *International Journal of Biological Macromolecules, 164*, 1443–1450.

Zhang, X., Aweya, J. J., Huang, Z. X., Kang, Z. Y., Bai, Z. H., Li, K. H., … Cheong, K. L. (2020). *In vitro* fermentation of *Gracilaria lemaneiformis* sulfated polysaccharides and its agaro-oligosaccharides by human fecal inocula and its impact on microbiota. *Carbohydrate Polymers, 234*, Article 115894.

Zhang, X., Liu, Y., Chen, X.-Q., Aweya, J. J., & Cheong, K.-L. (2020). Catabolism of *Saccharina japonica* polysaccharides and oligosaccharides by human fecal microbiota. *LWT-Food Science and Technology, 130*, Article 109635.

Zhou, X., Zhang, Z., Huang, F., Yang, C., & Huang, Q. (2020). *In vitro* digestion and fermentation by human fecal microbiota of polysaccharides from flaxseed. *Molecules, 25*(19), 4354.